# Photoinduced phenomena and structural analysis associated with the spin-state switching in the $[Fe^{II}(DPEA)(NCS)_2]$ complex

D. Glijer,[1,2] J. Hébert,[1] E. Trzop,[1] E. Collet,[1,2] L. Toupet,[1] H. Cailleau,[1,2] G. S. Matouzenko,[3] H. Z. Lazar,[4] J. F. Létard,[4] S. Koshihara,[2,5] and M. Buron-Le Cointe[1,2,*]

[1]*Institut de Physique de Rennes, Université de Rennes 1-CNRS, UMR 6251, Bâtiment 11A Campus de Beaulieu, 35042 Rennes, France*

[2]*ERATO, Japan Science and Technology Agency, 3-5 Sanbanchou, Chiyoda-ku, Tokyo 102-0075, Japan*

[3]*Laboratoire de Chimie, CNRS-Ecole Normale Supérieure de Lyon, UMR 5182, 46 allée d'Italie, 69364 Lyon Cédex 07, France*

[4]*CNRS, ICMCB, Université Bordeaux I, 87 Avenue du Docteur A. Schweitzer, 33608 Pessac, France*

[5]*Tokyo Institute of Technology, 2-12-1 Oh-okayama, Meguro-ku, Tokyo 152-8551, Japan*

(Received 17 March 2008; revised manuscript received 9 September 2008; published 29 October 2008)

Out-of-equilibrium photoinduced switching from the low-spin to the high-spin state has been investigated on the iron(II) complex $[Fe^{(II)}(DPEA)(NCS)_2]$ by both optical reflectivity and magnetic measurements under continuous light irradiation at low temperature. The photoinduced HS state can be observed up to 47 K and the relaxation process has been followed. Structural changes of both the temperature- and the photoinduced spin-state switching have been analyzed in detail by x-ray diffraction indicating no change of symmetry. Short intermolecular contacts and intramolecular deformations associated with the change of molecular spin state have been quantified. Actually a crossover behavior is observed at thermal equilibrium with however a quasiabrupt shape indicating significant cooperative effects. These aspects are compared between the temperature- and photoinduced spin crossovers.

DOI: 10.1103/PhysRevB.78.134112 PACS number(s): 61.50.Ks, 05.70.Ln, 76.60.Es

## I. INTRODUCTION

Spin crossover molecular compounds are of major interest in both condensed-matter physics and chemistry as prototypes of cooperative molecular bistability related to the spin-state change between high-spin (HS) and low-spin (LS) states and with potential applications in photoswitching of materials.[1,2] In comparison with the behavior of spin crossover complexes in solution, in the solid state the molecular spin switching can be accompanied by feedback from intermolecular interactions. This manifests by a cooperative behavior and in some rare cases by a change of symmetry. Then, in case of isostructural changes, the switching at thermal equilibrium can occur through a first-order phase transition for large cooperative intermolecular interactions or through a crossover behavior for less cooperative ones. In other words, when there is no change of symmetry, the physical picture is similar to the liquid-gas phase transition below or above the critical point in the $(P,T)$ plane.[3] Thus the variation of the HS fraction as a function of temperature $T$ or pressure $P$ varies from gradual to abrupt with in this case a more or less wide hysteresis loop. Many theoretical works have addressed the origin of cooperativity in spin crossover materials in terms of elastic interactions as the molecular size changes depending on this spin state.[4–8] Besides equilibrium spin-state change, the discovery of the light-induced excited spin-state trapping (LIESST) effect[9] on $[Fe(ptz)_6](BF_4)_2$ under continuous light irradiation at low temperature and the reverse-LIESST effect[10] have been particularly exciting. A long lifetime of the excited species, as this occurs at low temperature below the temperature $T$(LIESST),[11,12] is the crucial point to induce photoswitching under continuous light irradiation so that it can be observed under weak excitation[1,2] typically a few mW $cm^{-2}$. It is much more recently that the effect of pulsed laser excitation started to be investigated.[13] In a similar way that at thermal equilibrium, such photoinduced molecular transformation manifests through dynamical phase transition or crossover[14,15] opening new routes for out-of-equilibrium cooperative phenomena and this new field of physics is rapidly progressing. Like at thermal equilibrium, the out-of-equilibrium spin-state change can be observed and characterized by investigating various physical properties: magnetic measurements which give direct information on the spin state and optical reflectivity or transmission measurements which are very sensitive to the electronic state change associated with the spin-state switching. More recently structural studies which are well known for analyzing volume change and intra- or intermolecular deformations revealed essential for demonstrating the different mechanisms driven by the importance of cooperative effects: namely, a phase-separation process with domain formation[16] (dynamical phase transition) and a homogeneous process[17] (crossover) have been directly observed.

The light-induced effect opens new perspectives for applications in photoswitching devices[18] such as light-controlled high-density memories. Efforts are presently made in two directions: first, the search of new compounds bistable around room temperature with a large hysteresis in which light could control and change the spin state;[19,20] second, the search of compounds with high $T$(LIESST) value. For that purpose, particularly interesting is the attempt to predict the $T$(LIESST) from a relation between the temperature of spin-state change at thermal equilibrium $T_{1/2}$ and the $T$(LIESST). Thus, it could have been shown that for a large number of complexes, these two temperatures are linearly linked with a coefficient $T_0$ depending on the ligand nature[21,22] (monodentate, bidentate, and meridional tridentate) or formation of three-dimensional network solids. According to it, the $[Fe^{(II)}(DPEA)(NCS)_2]$ here studied, where DPEA [(2-

 

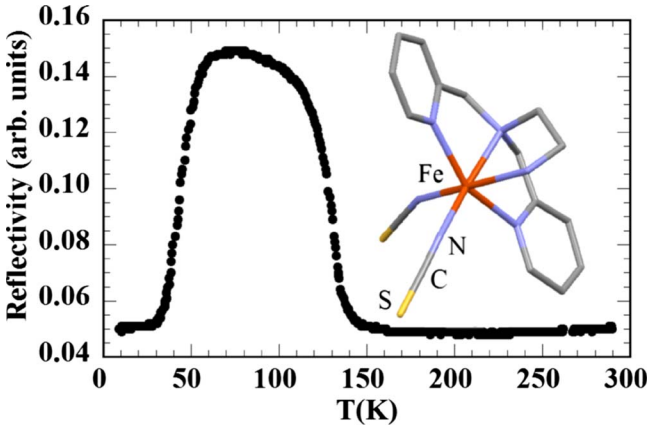


FIG. 1. (Color online) Reflectivity measurements probed at $\lambda = 800$ nm as a function of increasing temperature on $[Fe(DPEA)(NCS)_2]$. Insert: schematic representation of the $[Fe(DPEA)(NCS)_2]$ molecule (Hydrogen atoms are omitted for clarity).

aminoethyl)bis(2-pyridylmethyl)amine] is a tetradentate ligand (inset of Fig. 1), represents a promising candidate to obtain a high $T$(LIESST) value. Moreover, as this complex exhibits a thermal spin crossover at $T_{1/2}=138$ K,[23] we can expect to investigate a fascinating situation where $T$(LIESST) and $T_{1/2}$ values become close, that is, when the photoinduced metastable HS region and the stable thermal HS regime start to overlap. Such a special situation has been recently reported for another iron (II) spin crossover complex, and some very slow phase equilibrium has been recorded.[24]

The present paper is divided in three parts: the first one (Sec. III) details the photoinduced effects evidenced by reflectivity and magnetic measurements. The kinetics of the relaxation has been also followed, and the thermodynamic parameters have been determined. The second part (Sec. IV) is devoted to structural studies for both the spin-state change at thermal equilibrium (as a function of temperature) and out of equilibrium. In particular the nature of the photoinduced spin-state change has been investigated. Then the third part (Sec. V) is devoted to discussion: intermolecular interactions are evaluated at thermal equilibrium using a mean-field approach and the large similarities between equilibrium and out-of-equilibrium concerning the mechanisms of the spin-state switching are presented. Finally, we propose two reasons for explaining the discrepancies between the observed low $T$(LIESST) value and the expected high one.

## II. EXPERIMENTS

The $[Fe^{(II)}(DPEA)(NCS)_2]$ complex was obtained according to a procedure previously reported.[23] All the crystals used were selected from the same batch.

For investigating the LIESST *effect*, the measurement of the diffuse absorption spectra and reflectivity signal were performed by using a custom-built setup equipped with a SM240 spectrometer (Opton Laser International). This equipment allows recording of both the absorption spectra within the range of 500–900 nm at a given temperature and the temperature dependence (5–29 K) of the reflectivity signal at a selected probe wavelength (here $\lambda = 800$ nm $\pm 2.5$ nm; a few mW cm$^{-2}$). The diffuse reflectance spectrum was calibrated with respect to charcoal activated (Merck) as black standard and barium sulfate ($BaSO_4$, Din 5033, Merck) as white standard.

The photomagnetic measurements were performed using a Spectrum Physics Series 2025 $Kr^+$ laser ($\lambda = 647$ nm) or a laser diode ($\lambda = 830$ nm) coupled via an optical fiber to the cavity of a MPMS-55 Quantum Design superconducting quantum interference device (SQUID) magnetometer. The optical power at the sample surface was adjusted to 5 mW cm$^{-2}$, and the absence of change in magnetic response due to heating of the sample has been verified. Photomagnetic samples consisted of a thin layer of compound whose weight was obtained by comparison of the thermal spin crossover curve with that of a more accurately weighed sample of the same material. Our previously published standardized method for obtaining LIESST data was followed.[11,12] After cooling slowly to 10 K the sample, then in the low-spin state, was irradiated and the change in magnetism followed. Once the saturation point was reached the laser was switched off. The temperature was then raised at a rate of 0.3 K min$^{-1}$, and the magnetization was measured every 1 K.

Structural investigations at thermal equilibrium and under continuous light irradiation ($\lambda = 808$ nm 9.5 mW/cm$^2$) have been made by x-ray diffraction on single crystals. Data were collected on a four-circle Oxford diffraction Xcalibur 3 diffractometer (Mo $K_\alpha$ radiation) with a two-dimensional (2D) Sapphire 3 charge-coupled device (CCD) detector on needle shape samples with typical sizes around $300 \times 100 \times 100$ $\mu$m$^3$ in different experimental conditions. The single crystals were mounted either in an Oxford diffraction Helijet helium-flow cryostat allowing reaching 15 K or in an Oxford cryosystems nitrogen-flow cryostat allowing a better control of the temperature down to 78 K. The unit-cell parameters and the data reduction were obtained with CRYSALIS software from Oxford diffraction.[25] The structures were solved with SIR-97 (Ref. 26) and refined with SHELXL97.[27] Typical results of the structure refinement of the stable and photoinduced states gave final $R$ factor $0.0288 < R < 0.0438$.[28]

## III. PART I: OBSERVATION OF PHOTOINDUCED EFFECTS AT LOW TEMPERATURE AND KINETICS OF RELAXATION

Photoinduced effects have been searched down to 10 K both by following the change of the reflectivity signal at the surface of the sample and the magnetic response in bulk conditions. As absorption spectra in the visible region 500–850 nm show a large difference around 800 nm, this wavelength was chosen for the measurement of reflectivity under constant light irradiation from 10 to 300 K (Fig. 1). The increase in the diffuse reflectivity signal at around 138 K indicates the decrease in the absorption associated with the thermal HS $\rightarrow$ LS conversion. Indeed for iron(II) spin crossover complexes involving large aromatic ligand, such as

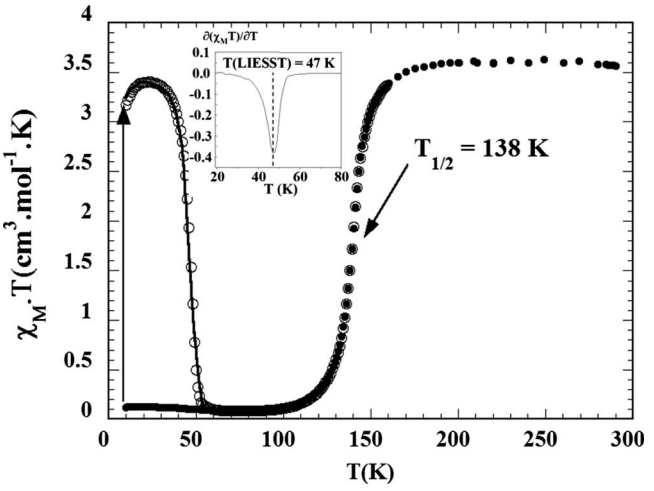


FIG. 2. Bottom: Magnetic-susceptibility measurements in the form $\chi_M \cdot T$ as a function of the temperature $T$ where $\chi_M$ is the magnetic susceptibility. Data collected at thermal equilibrium are represented by dark circles. Open circles (○) represent data registered after a laser irradiation made at 10 K (schematized by a continuous black arrow) during around 1 h, then stopped before a temperature increase (0.3 K min$^{-1}$). The black line is the simulation of the curve under irradiation by using the fitted kinetic parameters $E_a$(330 cm$^{-1}$), $k^{\infty}_{HL}$(38 s$^{-1}$), $k_{HL}(T \rightarrow 0)=5.10^{-5}$ s$^{-1}$, Landé factor $g=2.25$, $n_{HS}=1$, and $n_{LS}=0.05$. Insert: Derivative of the curve obtained under light irradiation and the minimum defines the $T$(LIESST) equal to 47 K (Refs. 11 and 12).

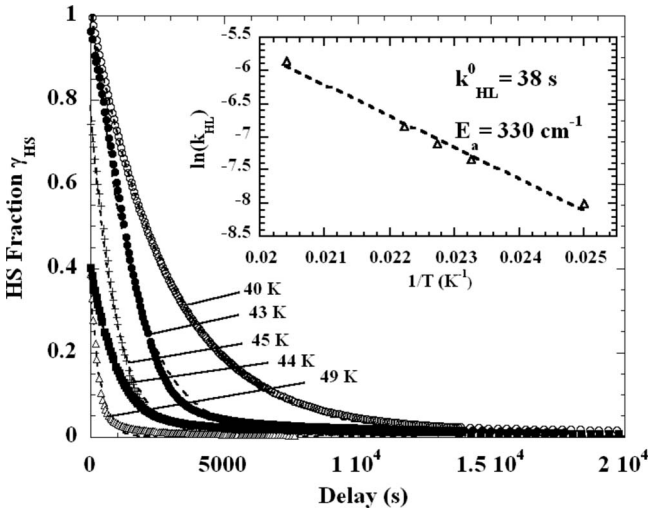


FIG. 3. Relaxation of the HS fraction as a function of temperature. Each time, the sample is first irradiated at 10 K where the complete transformation is achieved before the temperature is increased up to the desired temperature and the laser is switched off. The insert illustrates the determination (by the fitted curves in dashed lines) of the kinetic parameters $E_a$ and $k^{\infty}_{HL}$ defined in the text.

DPEA unit, the absorption spectra are typically composed in the HS state (above the thermal spin conversion) by the weakly allowed *d-d* band occurring at 800–850 nm; while in LS state (below the thermal spin conversion) mainly the metal-to-ligand (MLCT)-LS (charge-transfer) band, which totally overlaps the weak *d-d* LS transition, is present at around 500–700 nm. Interestingly, a large reflectivity change is observed not only around $T_{1/2}=138$ K but also below 50 K. The diffuse reflectivity signal measured at very low temperature (10 K) similar to the one observed for the high-temperature HS state suggests a photoinduced spin-state conversion below 50 K. Magnetic susceptibility measurements confirm the HS photoinduced state of the molecules in this low-temperature range (Fig. 2). The sample introduced in the SQUID is completely transformed after 1 h of irradiation. The $T$(LIESST) is determined from the minimum of a $d\chi_M T/dT$ versus $T$ plot for the relaxation process:[11,12] $T$(LIESST)=47 K (Fig. 2). Several kinetic experiments were performed by photoexciting the sample to obtain the light-induced HS state at 10 K and then heating under continuous irradiation with red (λ=647.1–676.4 nm) or near infrared (λ=830 nm) light. In each case, when the established temperature was reached, as given in Fig. 3, the light irradiation was stopped and the relaxation into the low-spin state was followed for several hours. The time dependency of the HS molar fraction $\gamma_{HS}(t)$ is deduced from molar magnetic susceptibility $\chi_M$ through $\gamma_{HS}(t)=\frac{\chi_M \cdot T(t)}{(\chi_M \cdot T)_{HT}}$ where $(\chi_M \cdot T)_{HT}$ is the high-temperature limit of $\chi_M \cdot T$. We can immediately notice that the starting point of each curve does not always correspond to a state with 100% of HS state molecules on Fig. 3. If we consider that at temperature higher than 40 K the influence of the zero-field splitting of the photoinduced HS state is negligible, the result that the starting HS molar fraction is lower than the unity can be reasonably explained by the competition between the photoexcitation and the relaxation processes which becomes faster as the temperature increases. As illustrated on Fig. 3 with some selected kinetics, the HS molar fraction $\gamma_{HS}$ clearly depends on temperature and experimental curves can be well fitted with a single-exponential law as $\gamma_{HS}(t)=\gamma_0 \cdot \exp(-k_{HL} \cdot t)$ where $\gamma_0$ represents the limits of the HS fraction at time $t=0$, and the rate constant for the HS to LS conversion $k_{HL}$ depends on the temperature $T$ and on the activation energy $E_a$ according to $k_{HL}=k^{\infty}_{HL} \cdot \exp(-\frac{E_a}{k_B T})$. Such a first-order kinetics relaxation is observed in systems without cooperative effects; i.e., the photoinduced HS molecules relax down to their thermal equilibrium LS state in an independent way from each other. Above 49 K, the relaxation kinetics is so high that it cannot be measured with our SQUID equipment. The calculated curves are shown as dotted lines in Fig. 3. The apparent activation energy $E_a$ and the apparent pre-exponential factor $k^{\infty}_{HL}$ of the activated region are calculated from the straight line given by plotting $\ln(k_{HL})$ versus $1/T$ (see inset of Fig. 3). The obtained kinetic parameters $E_a \approx 330$ cm$^{-1}$ and $k^{\infty}_{HL} \approx 38$ s$^{-1}$ compared to those obtained on other iron (II) complexes[29–31] are quite high relative to values reported for the first-order kinetics relaxation being in the range 100–200 cm$^{-1}$ for $E_a$ and $1 \times 10^{-2}$–$1 \times 10$ s$^{-1}$ for the pre-exponential $k^{\infty}_{HL}$ parameter. This point is commented in the third part (Sec. V) with results obtained by x-ray diffraction.

An elegant way to test the validity of this model of relaxation is to use the fitted parameters to reproduce the experimental $T$(LIESST) curve.[22,31] Briefly, it is now well estab-

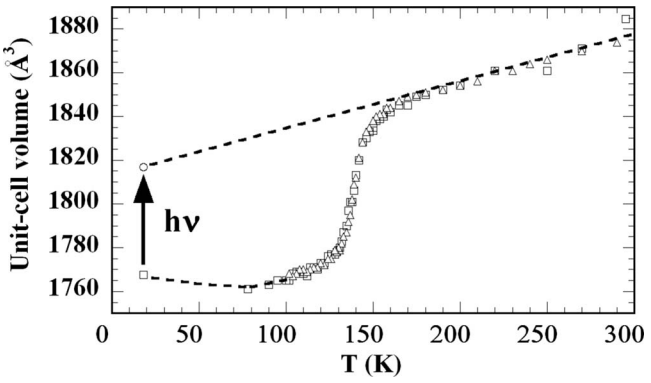


FIG. 4. Evolution of the unit-cell volume as a function of the temperature. Measurements made with increasing temperature are schematized with open triangles (△), whereas those made under cooling are schematized with open squares (□). The arrow schematizes the laser irradiation (λ=808 nm) made at 18 K. Dashed lines are guides for eyes.

lished that the $T$(LIESST) curve combines the relaxation of both the tunneling and the thermally activated regions, and we have demonstrated that for a spin crossover system the time dependence of the HS fraction at temperature $T$ can be obtained by following the equation $\frac{d\gamma_{HS}}{dt}=-\boldsymbol{k}_{HL}(\boldsymbol{T})\cdot\gamma_{HS}$ with $\boldsymbol{k}_{HL}=\boldsymbol{k}_{HL}^{\infty}\cdot\exp(-\frac{E_a}{k_BT})$ in the thermally activated region. At lower temperature, i.e., in the quantum-mechanical tunneling region, the rate constant $k_0$ [i.e., $\boldsymbol{k}_{HL}(\boldsymbol{T}\rightarrow 0)$] which then characterizes the relaxation is estimated as the upper limit from the last complete kinetic measurement recorded at low temperature, i.e., 40 K (Fig. 3). The calculated curve is shown as solid line in Fig. 2. The agreement between the calculated and the experimental $T$(LIESST) curves is very good.

## IV. PART II: STRUCTURAL INVESTIGATIONS

Structural studies are essential to get information at the atomic level. At thermal equilibrium, i.e., without light irradiation, the unit-cell volume and lattice parameters show continuous evolutions without any hysteresis loop (Figs. 4 and 5) and reproduce the shape of the magnetic curve (this work and Ref. 23). The structural signatures fit well with the value of $T_{1/2}=138$ K. No symmetry breaking has been found so that the space group remains the monoclinic one $P2_1/c$, $Z=4$. Therefore, the spin-state change from HS to LS at $T_{1/2}$ is associated with a spin crossover and not with a phase transition. As observed for many Fe(II) complexes,[1] the isostructural change from the HS to LS state is associated with a decrease in the volume unit cell (about 60 Å$^3$ here; Fig. 4). Nevertheless, the stacking axis $\boldsymbol{c}$ of the $Fe^{(II)}(DPEA)(NCS)_2$ molecules increases around the temperature-induced spin crossover from about 0.12 Å (Fig. 5) around the spin crossover temperature being in direct relation to the intermolecular contacts. Indeed, a careful analysis of these contacts reveals different distances shorter than the sum of van der Waals radii (Table I). Their number increases as the temperature decreases and the new short contacts have their highest

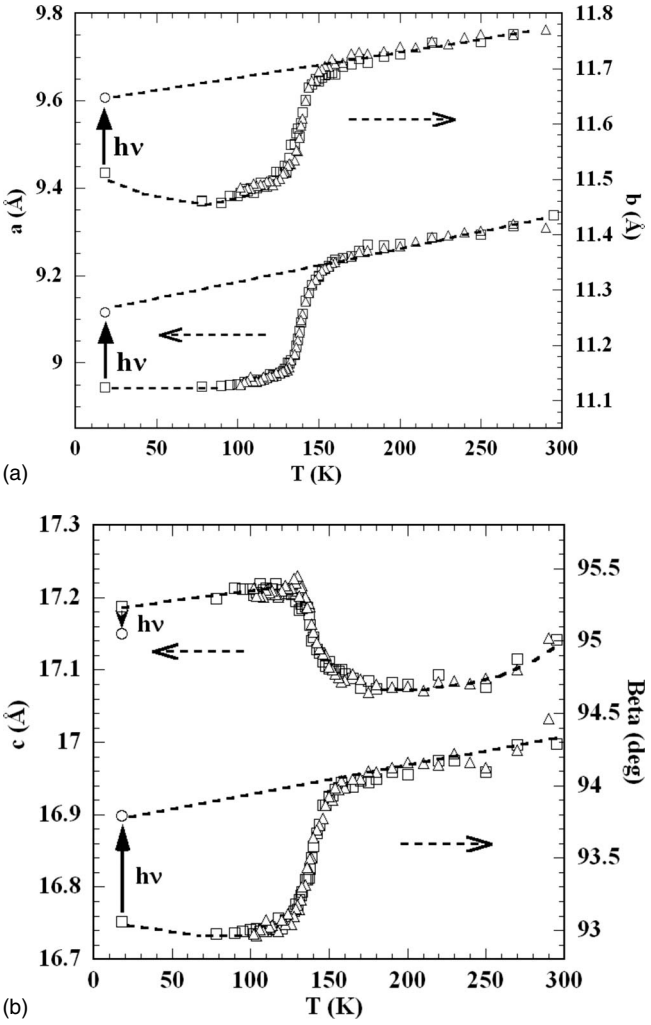


FIG. 5. Evolution of the unit-cell parameters as a function of the temperature. Measurements made with increasing temperature are schematized with open triangles (△), whereas those made under cooling are schematized with open squares (□). The arrows schematize the laser irradiation (λ=808 nm) made at 18 K. Dashed lines are guides for eyes.

component parallel to the $\boldsymbol{c}$ axis as illustrated on Fig. 7. Thus, to avoid the steric constraints due to very short intermolecular distances, the $\boldsymbol{c}$ cell parameter increases in the course of the spin crossover process. Besides, by considering the intermolecular Fe…Fe distances (Fig. 8), one can note that each of them from the first up to the fourth neighboring distances is characteristic of the spin state.

We discuss now the structural changes associated with the spin crossover from the intramolecular point of view. Here, the spin-state change manifests itself by the distortion of the $[FeN_6]$ octahedron.[32] Thus, the average $\langle$Fe-$N\rangle$ bond length of this octahedron decrease from about 2.16 Å for the HS state to around 1.98 Å in the LS one as typically observed in Fe(II) systems. In addition to the octahedron contraction associated with the change from less bonding HS to more bonding LS states, distortions of the octahedron are observed. On one hand, we define a parameter $\zeta$ as the deviation from this average $\langle$Fe-$N\rangle$ bond length: $\zeta=\Sigma_{i=1}^{6}|\text{Fe-}\boldsymbol{N}_i-\langle\text{Fe-}\boldsymbol{N}\rangle|$ is less important in the LS state than in the HS one

TABLE I. Average bond distances shorter than the sum of the van der Waals radii which are: S…H:3 Å, C…H:2.9 Å, H…H:2.4 Å, N…H:2.75 Å, C…C:3.4 Å, and S…C:3.5 Å. Atomic numbering: each atom is labeled by a letter indicating the atom type and a number. For hydrogen atom H, the number is the number of the linked atom and letters A and B are used when 2 H are linked to the same atom. Example: H35A and H35B are the two H atoms linked to the carbon atom labeled C35.

| | | $T=290$ K | $T=150$ K | $T=78$ K | $T=18$ K Laser off | $T=18$ K Laser on |
|---|---|---|---|---|---|---|
| S…H(Å) | S1…H41 | | 2.992 | 2.994 | 2.991 | 2.967 |
| | S2…H53B | | | 2.917 | 2.944 | |
| | S1…H31 | | 2.968 | 2.868 | 2.864 | 2.905 |
| | S1…H6A | 2.745 | 2.669 | 2.607 | 2.608 | 2.649 |
| | S2…H6B | 2.729 | 2.690 | 2.774 | 2.760 | 2.667 |
| | S1…H45A | | | | 2.992 | |
| | S2…H32 | 2.972 | 2.960 | | | 2.969 |
| C…H(Å) | C31…H53A | | | 2.785 | 2.794 | 2.895 |
| | C1…H45A | | | 2.838 | 2.825 | 2.884 |
| | C2…H35A | 2.871 | 2.871 | 2.832 | 2.836 | 2.889 |
| | C40…H35B | | | 2.753 | 2.751 | 2.857 |
| | C43…H33 | | | 2.869 | 2.871 | 2.891 |
| | C1…H6A | 2.624 | 2.635 | 2.807 | 2.812 | 2.670 |
| | C2…H42 | | | | | 2.891 |
| H…H(Å) | H31…H53A | 2.359 | 2.306 | 2.275 | 2.289 | 2.291 |
| N…H(Å) | N2…H35A | 2.625 | 2.585 | 2.730 | 2.717 | 2.575 |
| C…C(Å) | C32…C32 | | | 3.293 | 3.306 | |
| S…C(Å) | S2…C30 | | 3.494 | 3.452 | 3.439 | 3.446 |

(Fig. 6). On the other hand, we can use the parameter $\Sigma$ (Refs. 32 and 33) that is the sum of the 12 cis $\phi$ angles in the coordination sphere: $\Sigma=\Sigma_{i=1}^{12}|90-\phi_i|$; it decreases from about 85° in the HS state down to less than 50° in the LS one (Fig. 6). The two parameters show that the $[FeN_6]$ octahedron is more regular for the LS state of the Fe atom.

The nature of the photoinduced spin-state change has been also investigated at 18 K where complete data collections have been performed both before and under weak laser excitations. There was no significant laser heating effect as verified by plotting the so-called Wilson graphs.[34]

Structural analysis at 18 K shows that the photoinduced HS state is similar to the thermal equilibrium HS one within the thermal contraction. Indeed either from the average unit-cell volume or from the first coordination sphere surrounding the Fe atom will the photoinduced state be obtained starting from the high-temperature HS state and considering a linear thermal contraction (Figs. 4 and 6). Such a situation has already been observed in other spin crossover systems either mononuclear[35,36] or binuclear ones.[37] From the intermolecular point of view (Table I and Fig. 8), one can easily also conclude to the occurrence of the photoswitching to the HS state: The short contacts significantly change going back to values close to those observed in the thermodynamically stable HS state (at 150 K for example) and the same observation can be done for Fe…Fe intermolecular distances.

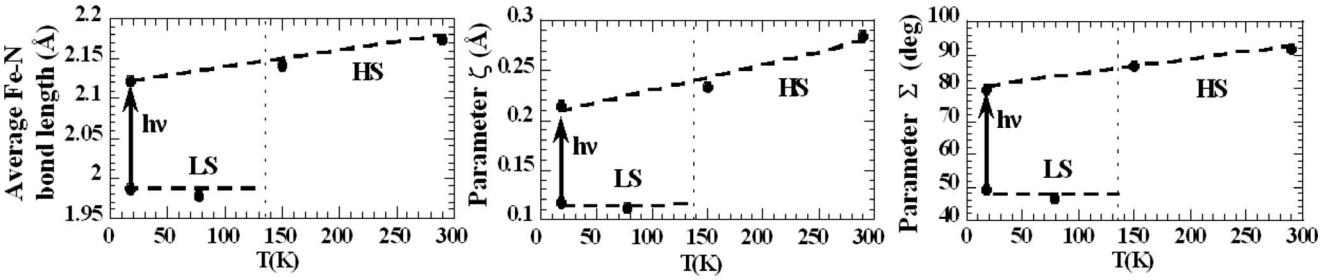


FIG. 6. Average bonding Fe-$N$ lengths (Å) (left), deviation from this average value defined as $\zeta=\Sigma_{i=1}^{6}|\text{Fe-}N_i-\langle\text{Fe-}N\rangle|$ (Å) (middle), and distortion of the $FeN_6$ octahedron measured from the $\Sigma$ parameter (Refs. 32 and 33) that is the sum of the 12 cis $\phi$ angles in the coordination sphere: $\Sigma=\Sigma_{i=1}^{12}|90-\phi_i|$ (right) as a function of temperature. The arrows schematize the laser irradiation made ($\lambda=808$ nm) at 18 K. Dashed lines are guides for eyes.

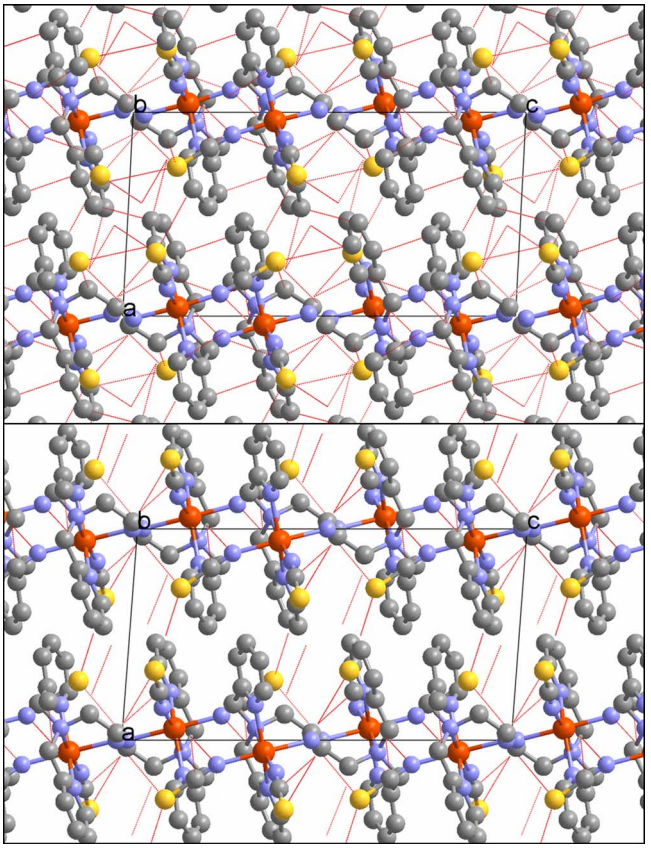


FIG. 7. (Color online) Short intermolecular contacts defined by distances shorter than the sum of van der Waals radii from structure resolution at 290 K (down) and 78 K (up). The ***c*** axis is the horizontal one, the ***a*** axis is the vertical one, and the ***b*** axis is perpendicular to the figure.

## V. PART III: DISCUSSION

Understanding how molecules couple in the solid to switch between different spin states and what are the key parameters driving the equilibrium and out-of-equilibrium spin conversion are present topic of interest.[3–8,14,15]

Let us first quantify the cooperativity of the system during temperature-induced spin crossover occurring at $T_{1/2}=138$ K through a mean-field approach.[38,39] Then, the molar free enthalpy $G$ of an assembly of molecules carrying one Fe(II) atom expresses itself as a function of the molar fraction of HS state $\gamma_{HS}$ and of a term of intermolecular interaction $\Gamma$ as

$$G = (1-\gamma_{HS})G_{LS} + \gamma_{HS}G_{HS} - TS_{mix} + \Gamma \cdot \gamma_{HS} \cdot (1-\gamma_{HS}), \tag{1}$$

where the mixing entropy $S_{mix}$ expresses as $S_{mix}=-R\cdot[\gamma_{HS}\cdot\ln(\gamma_{HS})+(1-\gamma_{HS})\cdot\ln(1-\gamma_{HS})]$ for an ideal solution. Zero energy is chosen for $G_{LS}$ so that $\Delta G=G_{HS}=\Delta H-T\Delta S$ where $\Delta H$ and $\Delta S$ are the enthalpy and the entropy variations associated with the spin-state change. These are related through $\Delta H=\Delta S\cdot T_{1/2}$. A value of $\Delta H=6760$ J mol$^{-1}$ has been determined by fittings of magnetic and Mössbauer spectroscopy measurements.[23] Equation (1) becomes

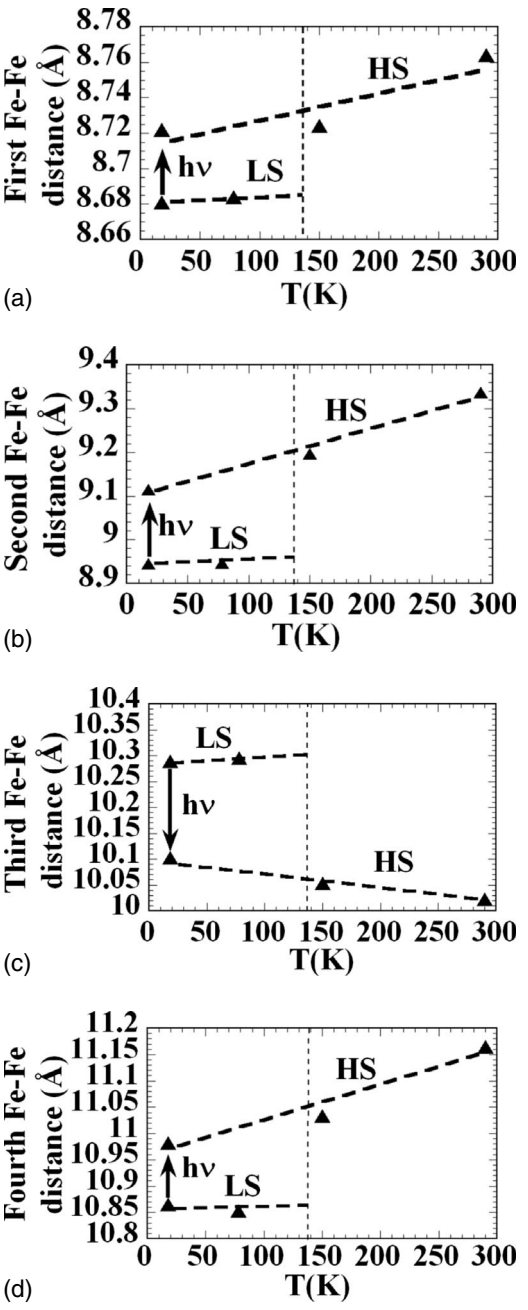


FIG. 8. Temperature evolution of the four shortest intermolecular Fe-Fe distances. The arrows schematize the laser irradiation made ($\lambda=808$ nm) at 18 K. Dashed lines are guides for eyes.

$$G = \gamma_{HS}\cdot\Delta H + \Gamma\cdot\gamma_{HS}\cdot(1-\gamma_{HS}) + RT\left(\gamma_{HS}\cdot\ln(\gamma_{HS}) + (1-\gamma_{HS})\cdot\ln(1-\gamma_{HS}) - \frac{\Delta S\cdot\gamma_{HS}}{R}\right).$$

Then, the evolution of $\gamma_{HS}$ as a function of the temperature $T$ only depends on the cooperativity parameter $\Gamma$ according to

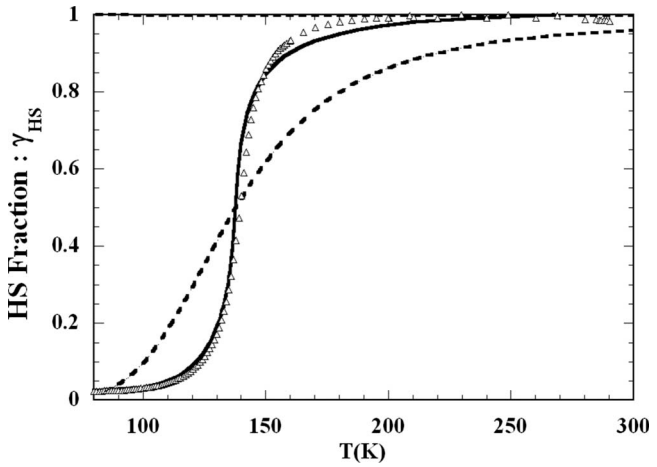


FIG. 9. Evolution of the HS molar fraction $\gamma_{HS}$ (showed with Δ) as a function of temperature $T$. The lines represent fitted curves with $T_{1/2}$ fixed to 138 K and $\Delta H$ is taken equal to 6760 J mol$^{-1}$ according to previous experiments (Ref. 23): the dashed line is the fit deduced from Eq. (2) when the intermolecular interaction term $\Gamma=0$ and the continuous line is a similar fit but adjusting a nonzero value for $\Gamma=2042\pm94$ J mol$^{-1}$ for fitting the experimental data.

$$T = \frac{\Delta H + \Gamma(1-2\gamma_{HS})}{R \ln\left(\frac{1-\gamma_{HS}}{\gamma_{HS}}\right) + \Delta S} \quad (2)$$

obtained from the equilibrium condition $(\frac{\partial G}{\partial \gamma_{HS}})_{T,P}=0$. Figure 9 shows that a value of $\Gamma\approx2050$ J mol$^{-1}$ (i.e., 164 cm$^{-1}$) for the intermolecular interaction parameter is necessary for fitting the experimental data according to this mean-field approach. The critical point $C$ is defined by $\Gamma_C=2RT_{1/2}(\approx2294$ J mol$^{-1}$). Here, $\Gamma$ is smaller than but very close to $\Gamma_C$. This model indicates that the spin-state change occurs in the hypercritical regime slightly above the critical point $C$. By analogy to the liquid-gas phase transition, it is not a first-order phase transition but a crossover with however quite significant cooperative effects because of the vicinity of the critical point $C$. It is in perfect agreement with the continuous but narrow evolution of signatures characteristic of the spin conversion such as volume (Fig. 4) and magnetic susceptibility (this work and Ref. 23): 90% of the spin-state change is situated in a 30 K temperature range (between 150 and 120 K). It is interesting here to underline the similarities from the cooperativity point of view between the thermal equilibrium and the out-of-equilibrium photoinduced spin crossovers. After light irradiation, the kinetics of relaxation (see Sec. III) follows exponential law which is qualitatively not different from independent molecular processes. However with regards to other spin crossover systems, the kinetic parameters values are quite high. This suggests the proximity of a sigmoidal behavior for this relaxation which always originates from cooperative effects.[14,15]

The present study shows that the $[Fe^{(II)}(DPEA)(NCS)_2]$ compound with DPEA as a tetradentate ligand does not present a high $T$(LIESST) value close to $T_{1/2}$ as expected by the virtual "$T_0=180$ K" line extrapolated from the behavior observed on systems with other ligand structure.[21,22] Up to now, four series of compounds have shown parallel "$T_0$ lines" with values of the coefficient $T_0=100$ K for Fe(II) complexes of monodentate ligands, 120 K for systems with bidentate ligands, 150 K for systems involving meridional tridentate ligands, and 200 K for 3D networks solids. Physical origin of $T_0$ is still uncertain but appears to primarily depend on the geometry and conformational rigidity of the ligand linked to the metal ion. Thus, some spin crossover complexes with tridentate ligands possessing some vibrational degrees of freedom carried by unsaturated carbon atoms between the aromatic ring present $T$(LIESST) values following the "$T_0=100$ K" line,[40,41] i.e., a $T$(LIESST) value which has decreased in comparison with the one observed on compounds with a more rigid ligand. Factors outside the inner metal coordination sphere such as intermolecular packing and the nature of any anions or solvent in the material would typically result in only minor perturbations of $T_0$ for a given set of metal complexes. From that point of view, the observations found here on $[Fe^{(II)}(DPEA)(NCS)_2]$ where the ligand DPEA possesses some flexible unsaturated carbon atom connecting the aromatic rings (insert of Fig. 1) show that it is a new example of nonoptimized ligand system in regard to the stabilization of the light-induced HS state. The high flexibility of the $[Fe^{(II)}(DPEA)(NCS)_2]$ molecules also manifests itself in the important entropy variation at $T_{1/2}$ and $\Delta S=49$ J·K$^{-1}$·mol$^{-1}$ significantly larger than the electronic contribution $\Delta S_e=R\ln15\approx22.5$ J·K$^{-1}$·mol$^{-1}$ (considering orbital and spin degeneracy[1]). It shows that an important contribution comes from vibrational part ($\Delta S_{vib}\approx26.5$ J.K$^{-1}$.mol$^{-1}$) and recent studies on other iron (II) compounds are in favor of a prominent contribution of the intramolecular vibrations (coordination core).[42–44] All these considerations are in favor of both vibrational aspects and hardness of the inner coordination sphere as being the key factors in the stabilization of the light-induced metastable HS state. However, Raman and IR spectroscopic measurements which would allow us to distinguish between the contributions of intramolecular and intermolecular vibrations to the entropy variation at $T_{1/2}$ are missing for the $[Fe^{(II)}(DPEA)(NCS)_2]$ compound. We can also not exclude that factor affecting the intermolecular packing can play a preponderant role on the stabilization of the HS state in some cases. From that point of view, an interesting lead is to carefully look for intermolecular packing on a large number of such compounds as polymorphs of spin crossover compounds can present very different behaviors either by varying the temperature[31,36,45] or under light irradiation.[31,36]

## VI. CONCLUSION

Spin-state switching has been investigated in details in the iron (II) complex $[Fe^{(II)}(DPEA)(NCS)_2]$: at thermal equilibrium, it is a spin crossover (no change of symmetry) occurring at $T_{1/2}=138$ K. Photoinduced effects ($\lambda=647$ and 808 nm) have been evidenced and characterized at the atomic level at low temperature [$T$(LIESST)=47 K]. The relaxation mechanism follows the exponential law observed for inde-

pendent molecules process not far however from a sigmoidal behavior. From this point of view, this out-of-equilibrium behavior presents strong similarities with the one observed at thermal equilibrium where a mean-field model allows to estimate an intermolecular interaction parameter just little weaker than the one corresponding to the critical point $C$, in agreement with the quite abrupt character of the crossover. Moreover, this work underlines the high flexibility of the DPEA ligand visible on the high vibrational part of the entropy variation at $T_{1/2}$. This flexibility may explain the low-unexpected $T$(LIESST) value observed in this compound but intermolecular interactions may also play an important role as demonstrated by studies on polymorphs of other complexes.

## ACKNOWLEDGMENTS

This work was partly supported by the European Node of Excellence (Grant No. NOE MAGMANet 515767-2), the European FLASH network (Grant No. MRTN-CT-2003-503641), the National Research Agency (ANR "Fast-switch" with Grant No. NT05-3-45333), the French ministry of research (ACI JC, E.C.), and the Région Bretagne (PRIR Femtocom 2178, SIE MagBreiz 2142, and Ph.D funding for J.H.). The authors are also grateful to the members of the GDR Magnétisme et Commutation Moléculaire (MCM 2007-2011) for fruitful and passionate discussions.

*Author to whom correspondence should be addressed. marylise.buron@univ-rennes1.fr

[1] P. Gütlich, A. Hauser, and H. Spiering, Angew. Chem. **33**, 2024 (1994).
[2] *Spin Crossover in Transition Metal Compounds*, edited by P. Gütlich and H. A. Goodwin (Springer-Verlag, Berlin, 2004), Vol. 1-3.
[3] K. Boukheddaden, I. Shteto, B. Hôo, and F. Varret, Phys. Rev. B **62**, 14796 (2000).
[4] H. Spiering, K. Boukheddaden, J. Linares, and F. Varret, Phys. Rev. B **70**, 184106 (2004).
[5] M. Nishino, K. Boukheddaden, Y. Konishi, and S. Miyashita, Phys. Rev. Lett. **98**, 247203 (2007).
[6] S. Miyashita, Y. Konishi, M. Nishino, H. Tokoro, and P. A. Rikvold, Phys. Rev. B **77**, 014105 (2008).
[7] Y. Konishi, H. Tokoro, M. Nishino, and S. Miyashita, Phys. Rev. Lett. **100**, 067206 (2008).
[8] K. Boukheddaden, M. Nishino, and S. Miyashita, Phys. Rev. Lett. **100**, 177206 (2008).
[9] S. Decurtins, P. Gütlich, C. P. Köhler, H. Spiering, and A. Hauser, Chem. Phys. Lett. **105**, 1 (1984).
[10] A. Hauser, Chem. Phys. Lett. **124**, 543 (1986).
[11] J. F. Létard, P. Guionneau, L. Rabardel, J. A. K. Howard, A. E. Goeta, D. Chasseau, and O. Kahn, Inorg. Chem. **37**, 4432 (1998).
[12] J. F. Létard, L. Capes, G. Chastanet, N. Moliner, S. Létard, J. A. Real, and O. Kahn, Chem. Phys. Lett. **313**, 115 (1999).
[13] E. Freysz, S. Montant, S. Létard, and J. F. Létard, Chem. Phys. Lett. **394**, 318 (2004).
[14] O. Sakai and T. Ogawa, in *Photoinduced Phase Transitions*, 1st ed., edited by K. Nasu (World Scientific, Singapore, 2004), Chap. 3, p. 117.
[15] K. Boukheddaden, I. Shteto, B. Horomano, and F. Varret, Phys. Rev. B **62**, 14806 (2000).
[16] N. Huby, L. Guérin, E. Collet, L. Toupet, J. C. Ameline, H. Cailleau, T. Roisnel, T. Tayagaki, and K. Tanaka, Phys. Rev. B **69**, 020101(R) (2004).
[17] A. Goujon, B. Gillon, A. Debede, A. Cousson, A. Gukasov, J. Jeftic, G. J. McIntyre, and F. Varret, Phys. Rev. B **73**, 104413 (2006).
[18] J. F. Létard, P. Guionneau, and L. Goux-Capes, Top. Curr. Chem. **235**, 221 (2004).
[19] S. Bonhommeau, G. Molnar, A. Galet, A. Zwick, J. A. Real, J. J. McGarvey, and A. Bousseksou, Angew. Chem., Int. Ed. **44**, 4069 (2005).
[20] S. Cobo, G. Molnar, J. A. Real, and A. Bousseksou, Angew. Chem., Int. Ed. **45**, 5786 (2006).
[21] J. F. Létard, P. Guionneau, O. Nguyen, J. S. Costa, S. Marcen, G. Chastanet, M. Marchivie, and L. Goux-Capes, Chem.-Eur. J. **11**, 4582 (2005).
[22] J. F. Létard, J. Mater. Chem. **16**, 2550 (2006).
[23] G. S. Matouzenko, A. Bousseksou, S. Lecocq, P. J. Van Koningsbruggen, M. Perrin, O. Kahn, and A. Collet, Inorg. Chem. **36**, 2975 (1997).
[24] V. A. Money, C. Carbonera, J. Elhaïk, M. A. Halcrow, J. A. K. Howard, and J. F. Létard, Chem.-Eur. J. **13**, 5503 (2007).
[25] CrysAlis RED, Oxford Diffraction Ltd, Version 1.171.32.5, 2007.
[26] A. Altomare, M. C. Burla, M. Camalli, G. Cascareno, C. Giacovazzo, A. Guagliardi, A. G. G. Moliterni, G. Polidori, and R. Spagna, J. Appl. Crystallogr. **32**, 115 (1999).
[27] G. M. Sheldrick, SHELX97, program for the Refinement of Crystal Structures, University of Göttingen, Germany, 1997.
[28] CCDC-68105 up to CCDC-681019 contains the supplementary crystallographic data for this paper. These data can be obtained free of charge via www.ccdc.cam.ac.uk/conts/retrieving.html [or from the Cambridge Crystallographic Data Centre, 12 Union Road, Cambridge CB21EZ, UK; Fax: (44)–1223–336033; or deposit@ccdc.cam.uk)]
[29] L. Capes, J. F. Létard, and O. Kahn, Chem.-Eur. J. **6**, 2246 (2000).
[30] T. Buchen, P. Gütlich, K. H. Sugiyarto, and H. A. Goodwin, Chem.-Eur. J. **2**, 1134 (1996).
[31] J. F. Létard, G. Chastanet, O. Nguyen, S. Marcen, M. Marchivie, P. Guionneau, D. Chasseau, and P. Gütlich, Monatsch. Chem. **134**, 165 (2003).
[32] M. Marchivie, P. Guionneau, J. F. Létard, and D. Chasseau, Acta Crystallogr., Sect. B: Struct. Sci. **59**, 479 (2003).
[33] P. Guionneau, C. Brigouleix, Y. Barrans, A. E. Goeta, J. F. Létard, J. A. K. Howard, J. Gaultier, and D. Chasseau, C.R. Acad. Sci., Ser. IIc: Chim **4**, 161 (2001).
[34] See EPAPS Document No. E-PRBMDO-78-016837 for expla-

nation about the method and for seeing Wilson graphs. For more information on EPAPS, see http://www.aip.org/pubservs/epaps.html.

[35] M. Marchivie, P. Guionneau, J. F. Létard, D. Chasseau, and J. A. K. Howard, J. Phys. Chem. Solids **65**, 17 (2004).

[36] J. Hébert, N. Moisan, M. Lorenc, M. Buron-Le Cointe, L. Toupet, J.-F. Létard, P. Guionneau, E. Freysz, H. Cailleau, and Eric Collet (unpublished).

[37] E. Trzop, M. Buron-Le Cointe, H. Cailleau, L. Toupet, G. Molnar, A. Bousseksou, A. B. Gaspar, J. A. Real, and E. Collet, J. Appl. Crystallogr. **40**, 158 (2007).

[38] C. P. Slichter and H. G. Drickamer, J. Chem. Phys. **56**, 2142 (1972).

[39] A. Hauser, J. Jeftic, H. Romstedt, R. Hinek, and H. Spiering, Coord. Chem. Rev. **190-192**, 471 (1999).

[40] C. Enachescu, J. Linares, F. Varret, K. Boukheddaden, E. Codjovi, S. G. Salunke, and R. Mukherjee, Inorg. Chem. **43**, 4880 (2004).

[41] S. Bonhommeau, N. Bréfuel, V. K. Palfi, G. Molnar, A. Zwick, L. Salmon, J. P. Tuchages, J. S. Costa, J. F. Létard, H. Paulsen, and A. Bousseksou, Phys. Chem. Chem. Phys. **7**, 2909 (2005).

[42] G. Brehm, M. Reiher, and S. Schneider, J. Phys. Chem. A **106**, 12024 (2002).

[43] J. P. Tuchages, A. Bousseksou, G. Molnar, J. J. McGarvey, and F. Varret, Top. Curr. Chem. **235**, 85 (2004).

[44] Y. Miyazaki, T. Nakamoto, S. Ikeuchi, K. Saito, A. Inaba, M. Sorai, T. Tojo, T. Atake, G. S. Matouzenko, S. Zein, and S. A. Borshch, J. Phys. Chem. B **111**, 12508 (2007).

[45] G. S. Matouzenko, A. Bousseksou, S. Lecocq, P. J. Van Koningsbruggen, M. Perrin, O. Kahn, and A. Collet, Inorg. Chem. **36**, 5869 (1997).